Developmental and Comparative Immunology 92 (2019) 116–128

Contents lists available at ScienceDirect

Developmental and Comparative Immunology

journal homepage: www.elsevier.com/locate/devcompimm

Insights into the dynamics of memory, effector and apoptotic cytotoxic T lymphocytes in channel catfish, *Ictalurus punctatus*

David A. Spencer[a,1], Sylvie M.A. Quiniou[b], Jonathan Crider[a], Bryan Musungu[b], Eva Bengten[a], Melanie Wilson[a,*]

[a] Department of Microbiology and Immunology, University of Mississippi Medical Center, Jackson, MS, 39216, USA
[b] Warmwater Aquaculture Research Unit, U.S. Department of Agriculture-Agricultural Research Service, Stoneville, MS, 38776, USA

ARTICLE INFO

Keywords:
Effector T cells
Memory T cells
Natural IgM
Lipid binding
Phosphatidylinositol bisphosphate
Teleosts

ABSTRACT

In this study, we used the channel catfish model clonal TS32.15 alloantigen-specific cytotoxic T cell (CTL) line to examine the dynamics of memory CTL expansion and senescence in teleosts. Although TS32.15 has been routinely cultured to study catfish CTL responses and killing mechanisms, little is known about the dynamics of the CTLs in these cultures. Here we show that this cell line consists of small non-cytotoxic T cells and larger granular effector T cells and that their ratios vary with time after stimulation. Small CTLs, when exposed to their irradiated targets, replicate and differentiate to morphologically distinct cytotoxic effectors, which do not replicate. After lysing target cells, or with prolonged absence of stimulation, the effector cells transition to a non-cytolytic senescent stage or become apoptotic. In addition, we demonstrate that natural IgM in catfish serum binds lipids, including PIP_2, on early apoptotic CTLs, and that these IgM^+ CTL can be cleared by catfish head kidney-derived macrophages.

1. Introduction

Cytotoxic T Lymphocytes (CTLs) are well studied in mice and humans, and differentiation of effector and memory CTLs has been examined *in vitro* using both mixed leukocyte cultures (MLCs) and clonal CTLs. Clonal CTL lines require regular stimulation by antigen presenting cells that express their cognate peptide antigen-MHC complexes and cytokine growth factors (IL-2 and/or IL-15, reviewed in Cornish et al., 2006). As such, and over the past 30 years, the use of these culture systems and long-term clonal CTLs have not only defined CTL effector mechanisms, but more recently enabled researchers to examine CTL differentiation and effector cell killing rates. For example, Vasconcelos et al. (2015) demonstrated that intra-clonal heterogeneity in killing performance occurs in human $CD8^+$ CTL clones. Specifically, the use of time-lapse microscopy in combination with bulk or single cell killing assays revealed that only 34% of CTLs exhibit a high killing rate. Interestingly, sub-cloning of high-rate and low-rate killer cells yielded progeny cultures that exhibited a similar heterogeneity to the original CTL clones. The authors classified these CTLs as effector memory cells based on their expression of CD45RO, CCR7, CD27, CD28, IL-7Rα, PD-1, and perforin (Vasconcelos et al., 2015).

In another study, using transgenic mice and *in vitro* cultures, Kinjyo et al., in 2015 examined the correlation between $CD8^+$ CTL proliferation and differentiation fate by using a cell cycle fluorescent protein reporter system, which allowed real-time tracking of cell cycle dynamics (Kinjyo et al., 2015). These assays, when used to examine virus-specific $CD8^+$ CTLs *in vivo* and *in vitro*, showed that cycling during the first cell divisions after antigen stimulation were fast and uniform. However, after eight cell divisions a population of slow- or non-dividing CTLs appeared (cell division time was > 24hrs). These slower dividing CTLs were $CD62L^{hi}$ and smaller in size as compared to the faster dividing cells that were larger and $CD62L^{lo}$. In addition, microarray analyses demonstrated that the smaller cells expressed transcripts for chemokine receptors (CCR7 and CXCR3) and transcription factors TCF1 and ELF4, which are important for memory $CD8^+$ T cells development and function. As expected, the larger size CTLs expressed perforin and granzymes, and cell cycle regulators associated with proliferation. Notably, the authors demonstrated in adoptive transfer experiments that rapidly dividing effector cells could give rise to both effector and memory cell populations even at later time points after multiple division cycles.

In this regard, here we use the catfish model TS32.15 CTL line in the context of examining CTL proliferation and differentiation. The

* Corresponding author.
E-mail address: mwilson@umc.edu (M. Wilson).
[1] Present address: David A. Spencer, Division of Pathology & Immunology, Oregon Health and Science University, Beaverton, Oregon 97006.

https://doi.org/10.1016/j.dci.2018.11.001
Received 30 September 2018; Received in revised form 3 November 2018; Accepted 3 November 2018
Available online 14 November 2018
0145-305X/

alloantigen-dependent TS32 CTL lines were first cloned from mixed leukocyte culture (MLC) established from peripheral blood leukocytes (PBLs) collected from a fish hyper-immunized with allogenic catfish 3B11 B cells (Stuge et al., 2000). TS32.15 CTLs kill efficiently at low effector to target ratios (0.25:1) and kill exclusively by the secretory perforin and granzyme pathway, i.e. their killing was completely inhibited by EGTA or treatment with concanamycin. Also, TS32.15 exhibits strict alloantigen specificity for 3B11s (Zhou et al., 2001). TS32.15 CTL do not express message for CD8 or CD4 co-receptor molecules, however, they do express lymphocyte specific protein tyrosine kinase (Lck) and CD2, and their interaction, is predicted to allow the phosphorylation of CD3 that initiates TS32.15 signal transduction (Edholm et al., 2007; Taylor et al., 2015).

As detailed in this study, clonal TS32.15 T cell cultures contain both small non-cytotoxic cells and large granular effector cells. After stimulation with irradiated target cells, the small CTLs replicate and differentiate to the morphologically distinct larger cytolytic effectors that do not replicate. These effectors, after killing their targets or in the absence of stimulation, transition to a senescent stage or become apoptotic. Interestingly, natural IgM acquired from the catfish serum used to supplement the culture media binds to lipids on these small early apoptotic CTLs, and this provides the means to discriminate between memory and senescent small CTLs.

2. Materials and methods

2.1. Experimental animals, lymphocyte isolation and tissue collection

All fish were handled in accordance with national regulatory guidelines and approved by the UMMC Institutional Animal Care and Use Committee (IACUC). Outbred channel catfish obtained from the Warmwater Aquaculture Research Unit in Stoneville, MS (USDA-Agricultural Research Service) were individually housed as described (van Ginkel et al., 1992). For collection of PBLs, fish were anesthetized with tricaine methanesulfonate (MS-222; Western Chemical Inc) and ≤8 mls blood was drawn from the caudal vein using heparinized collection tubes. The collected whole blood was diluted 1:3 with RPMI adjusted to catfish tonicity with 10% (v/v) H_2O and layered over a cushion of Ficoll-Hypaque (Accurate Chemical) as previously described (Miller et al., 1994a). For tissue collection, fish were sacrificed with tricaine overdose and tissues harvested under sterile conditions.

2.2. Catfish cells

Catfish cell lines were grown from freezer stocks maintained in FBS with 10% DMSO at −80 °C by the laboratory. Frozen cells were washed twice with sterile RPMI and resuspended in growth media. All catfish cells were grown at 27 °C with 5% CO_2 and 100% humidity. The catfish clonal autonomous B cell (3B11 and 1G8) and T cell (28S.3 and G14D) lines were grown in AL-4 medium, consisting of equal parts L-15 and AIM-V media (Invitrogen) adjusted to catfish tonicity with 10% (v/v) H_2O and supplemented with 1 μg/ml $NaHCO_3$, 50 U/ml penicillin, 50 μg/ml streptomycin, 50 μM 2-ME and 4% heat inactivated catfish serum (Hogan et al., 1999; Miller et al., 1994a, 1994b; Wilson et al., 1997, 1998a). 42 TA is a catfish non-clonal macrophage line that contains some T cells (Vallejo et al., 1991; Wilson et al., 1998b). The clonal TS32.15 CTLs were grown in AL-5 conditioned medium, which is similar to AL-4 except supplemented with 5% heat inactivated catfish serum, and 5% 42 TA and 5% 28S.3 culture supernatants as a source of growth factors. The TS32.15 CTL line is non-autonomous and requires weekly stimulation with ~1:1 ratio of irradiated 3B11 (6000 rads) for continuous growth (Stuge et al., 2000). TS32.15 cultures for this project were discarded after 14 stimulation cycles.

2.3. Growth and purification of mAbs

The mouse mAbs used in this study were anti-catfish IgM, 9E1 (isotype IgG_1, κ) reacts with the Igμ chain (Miller et al., 1987), anti-catfish IgL 3F12 (isotype IgG_1, κ) reacts with the IgL-F isotype (Lobb et al., 1984), anti-catfish IgL 11A2 (isotype IgG_{2b}, κ) reacts with the IgL-G isotype (Lobb et al., 1984), the mAb 3B6 (isotype IgM, κ) reacts with an unknown marker found only on 3B11 B cells and anti-trout IgM 1.14 (isotype IgG_1, κ) which was used as an isotype control and reacts with rainbow trout Igμ (Deluca et al., 1983). Hybridomas producing these mAbs were grown in advanced DMEM media supplemented with 15% heat inactivated FBS, and 50 U/ml penicillin. Supernatants were collected every 5–7 days; IgG isotypes were stored at −20 °C and IgM isotype were stored for up to 2 months at 4 °C.

2.4. Flow cytometry

For flow cytometry analysis, ~1×10^5 cells were transferred to each flow tube, washed with catfish RPMI, and incubated in 50 μl mouse hybridoma supernatant for 30 min on ice. Treated cells were then washed, resuspended in the appropriate goat anti-mouse secondary antibody-conjugate diluted in 50 μl catfish RPMI/1% BSA and incubated for 30 min on ice. Cells were then washed and resuspended in 250 or 500 μl catfish RPMI/1% BSA for analysis. Dilutions for secondary antibody conjugates were: 0.00625 μg/μl anti-IgM:PE (1:80 of 0.5 μg/μl stock), 0.005 μg/μl anti-IgG_1:APC (1:100 of 0.5 μg/μl stock), and 0.025 μg/μl anti-IgG_{2b}:FITC (1:40 of 1.0 μg/μl stock; Southern Biotech).

For assays measuring apoptosis, cells were stained for the presence of IgM as described above, then incubated with annexin V and propidium iodide using the Tali Apoptosis Kit (Molecular Probes). Briefly, ~1×10^6 cells were washed twice in catfish PBS, resuspended in 100 μl of the provided annexin binding buffer, and incubated for 20 min with 5 μl annexin V conjugated to AlexaFlour-488 at 25 °C protected from light. Cells were then washed, resuspended in 100 μl binding buffer, and 1 μl of the provided propidium iodide (PI) was added. After 5 min, cells were transferred directly to flow cytometry tubes containing 200 μl RPMI. All cells were analyzed on a NovoCyte 3000 Flow Cytometer (ACEA Biosciences) using a threshold of 10,000. In addition to the gating strategies described in the figure legends, residual noise ($< 10^3$ FSC-H, $< 10^3$ SSC-H) and doublets (using the SSC-A vs. SSC-H line) were gated out.

2.5. Cell cycle analysis

TS32.15 CTLs were fixed with 3% formaldehyde in PBS for 20 min at 25 °C, washed three times with PBS and incubated in 90% methanol for 1 h at −20 °C. Fixed and permeabilized cells were pelleted (1500 x g for 5 min), washed, and resuspended in binding buffer (Molecular Probes), before adding propidium iodide (1 μl/100 μl buffer). After 5 min, propidium iodide treated cells were transferred to flow cytometry tubes and analyzed.

2.6. RNA isolation and RT-PCR

Total RNA was extracted from freshly isolated PBL and TS32.15 CTLs at 10 days post stimulation, when irradiated 3B11 target cells were no longer present, using the RNAqueous-4PCR total RNA extraction kit (Ambion Life Technologies) and treated with DNase I according to the manufacturer's directions. cDNA was synthesized from ~2 to 10 μg RNA (generally 11 μl of total RNA resuspended in 15 μl) using an oligo(dT) primer and 200 U Superscript III reverse transcriptase (Invitrogen). RT-PCR was performed using gene specific primers (Supplemental Table 1) and GoTaq polymerase (Promega) according to the manufacturer's directions. The PCR amplification parameters were: 95 °C for 5 min, followed by 32 cycles of 95 °C for 30 s, 58 °C for 30 s, and 72 °C for 1 min, followed by 72 °C for 5 min.

2.7. ^{51}Cr release cytotoxicity assays

Cytotoxicity assays were performed as previously described by Yoshida et al. (1995). Briefly, 3×10^6 3B11 target cells were washed and labeled with 0.25 mCi $Na_2{}^{51}CrO_4$ (PerkinElmer) for 1.5 h under growth conditions (AL-5 media, 27 °C, 5% CO_2, and 100% humidity), washed twice, and incubated for an additional 30 min in AL-5. Targets were plated at 5×10^5 cells/100 µl/well in a 96 well round bottom plate and 100 µl of TS32.15 CTLs were added at the effector:target ratios indicated in the legend to Fig. 1. Plates were centrifuged at 200 x g for 2 min with low acceleration and brake, to induce contact between effectors and targets, then incubated for 4 h at 27 °C, 5% CO_2, and 100%

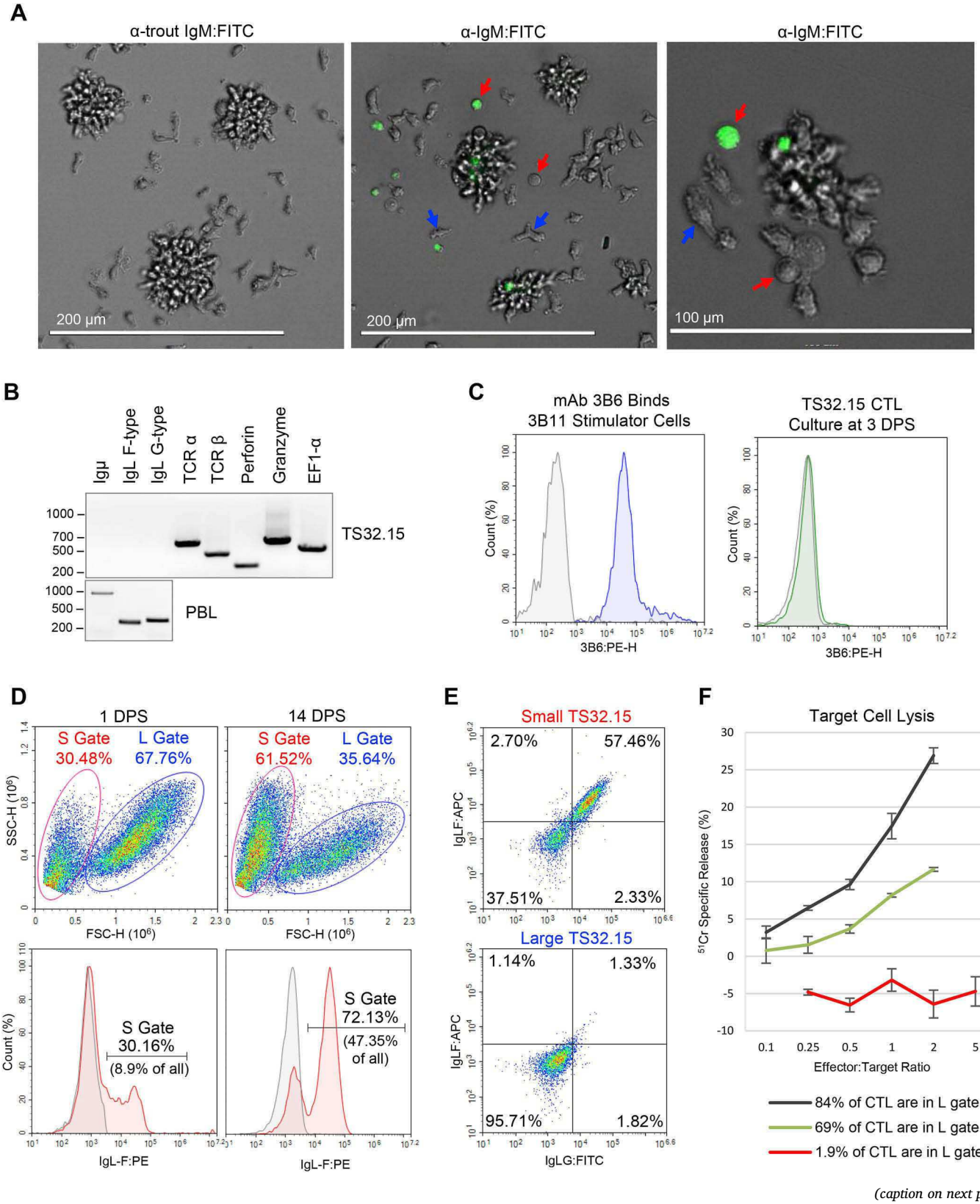

(caption on next page)

Fig. 1. TS32.15 is a non-synchronized catfish alloantigen specific CTL line and cultures contain small round cells that are IgM$^+$ and large elongated granular cells that are IgM$^-$. **(A)** Fluorescence microscopy overlays of TS32.15 CTLs at 5 DPS stained with anti-catfish IgM mAb 9E1 (green) or anti-rainbow trout IgM mAb 1.14 (isotype control) followed by goat anti-mouse IgG$_1$ conjugated to FITC. Red arrows indicate CTLs with a small round morphology, blue arrows indicate CTLs possessing a larger elongated morphology. Images are representative of 15 images collected from 3 independent experiments. **(B)** TS32.15 RNA was harvested at 10 days post stimulation (DPS) and RT-PCR was performed using specific primers for the membrane form of IgM, IgL-F, IgL-G, TCRα, TCRβ, granzyme B, and EF1-α as a control. Transcripts from catfish PBL (bottom panel) are shown as primer controls. Base pair markers (kb) are a left. Staining with mAb 3B6 prior to harvesting RNA confirmed 3B11 target cells were not present (data not shown). **(C)** TS32.15 CTLs at 3 DPS were stained with anti-catfish IgM mAb 9E1 or anti-rainbow trout IgM mAb 1.14 followed by goat anti-mouse IgG1:FITC. Staining with mAb 3B6 confirmed 3B11 target cells were not present (data not shown). **(D)** Scatter profiles of small and large TS32.15 CTL at day 1 DPS and at day 14 DPS are presented and their percentages are indicated above their gates. Histograms are shown for the small CTLs, which were stained with anti-catfish IgL-F mAb 3F12 followed by goat anti-mouse IgG:PE. The isotype control anti-rainbow trout IgM mAb 1.14 staining is in grey. The percentage of the small cells in the total culture is noted in the parentheses. **(E)** Scatter profile density plots of a representative TS32.15 culture at 5 days post stimulation stained for catfish IgL-F and IgL-G using mAbs 3F12 and 11A2 followed by anti-mouse IgG1:APC and IgG2b:FITC, respectively. The percentages of IgL-binding for TS32.15 CTLs gated on the small and large CTLs as defined by the S and L gates shown in panel D is indicated. Staining with mAb 3B6 confirmed that 3B11 target cells were not present (data not shown). **(F)** TS32.15 were FACS sorted using the S and L gates as shown in panel D, and the sorted TS32.15 CTLs were immediately plated in triplicate and used as effectors at the indicated E:T ratios, against ^{51}Cr-labeled 3B11 target cells. The mean specific release was calculated and is shown ± the standard error. The percentage of large TS32.15 CTLs present in each culture is indicated. Data is representative of three independent experiments. (For interpretation of the references to colour in this figure legend, the reader is referred to the Web version of this article.)

humidity. Following incubation, wells were mixed thoroughly by pipetting to ensure even distribution of ^{51}Cr in the media, and the cells were pelleted by centrifugation (500 x g for 5 min). One hundred µl of cell-free supernatant was removed from each well and cpm were determined using a COBRA II automatic gamma counter (Packard). Percent specific release was calculated according to the following formula:

$$\%\ \text{specific release} = \frac{(\text{cpm[experimental release]} - \text{cpm[spontaneous release]})}{(\text{cpm[maximum release]} - \text{cpm[spontaneous release]})} \times 100$$

Spontaneous release was defined as the average cpm of 6 wells containing targets incubated with 100 µl AL-5 instead of TS32.15 effector cells; for maximum release, 100 µl AL-5 containing 2% Triton was added to the targets instead of TS32.15 effectors. Average triplicate measurements for each effector to target ratio and their standard errors were calculated.

2.8. Immunofluorescence microscopy

TS32.15 CTLs, at 4 days post stimulation, were washed with catfish RPMI, resuspended in catfish PBS containing 3% formaldehyde and incubated for 20 min at 25 °C. The CTLs were then washed three times before resuspension in 50 µl 9E1 or 1.14 mAb hybridoma supernatant. After incubation for 60 min at 4 °C, the CTLs were washed twice then incubated with goat anti-mouse IgG$_1$:FITC (Southern Biotech) at a 1:25 dilution for 60 min at 4 °C. After incubation the CTLs were washed twice, resuspended in RPMI, and transferred to a 24 well plate for imaging using an EVOS® FL microscope (Life Technologies). For timelapse videos, TS32.15 CTLs at 6 days post stimulation were stained for IgM with mAb 9E1:FITC as described for flow cytometry, then incubated for 2 h in conditioned media with a 1:1 ratio of target 3B11 B cells labeled with CellTrace Far Red (Thermo Fisher Scientific). Initial fluorescent images were taken immediately prior to a 30 min brightfield timelapse where images were recorded every 10 s. Image files were assembled as timelapse videos in IMovie and uploaded as a Mendeley data set (Spencer, 2018).

2.9. Cell sorting and labelling

Prior to sorting, separate TS32.15 CTL cultures were grown to skew the populations towards the desired cell morphology, e.g. large effector cells, small IgM$^+$ or small IgM$^-$ cells, by adding different ratios of stimulator cells and harvesting the populations at different days after stimulation. For replication assays, cells were stained for IgM with mAb 9E1 followed by anti-mouse IgG$_1$:FITC as described for flow cytometry, then large IgM$^-$, small IgM$^+$, and small IgM$^-$ cells were FACS sorted with a MoFlow XDP cell sorter (Beckman Coulter). The sorted cell populations were immediately washed, resuspended in catfish PBS, pH-7.4, and labeled with CellTrace Violet (Thermo Fisher Scientific) according to the manufacturer's directions, using 1:1000 dye/DMSO dilution for 30 min at 28 °C. Following sorting and labeling, an aliquot of the cells was analyzed by flow cytometry to examine post-sort characteristics and the remaining cells were grown in conditioned media.

For RNAseq, strategically stimulated cultures were stained with 9E1 mAb followed by goat anti-mouse IgG$_1$:FITC and sorted using a FACS (MoFlow XDP). This method yielded pure IgM$^-$ populations, but failed to provide enough IgM$^+$ CTLs, so to obtain this population, a separate TS32.15 culture was stained with 9E1 followed by goat anti-mouse IgG$_1$:APC. These IgM$^+$ cells were MACS sorted with pre-coupled anti-APC magnetic beads using an EasySep isolation magnet (StemCell Technologies). MACS sorting was performed according to manufacturer's directions, with the exception that the anti-APC beads were washed four times prior to eluting IgM$^+$ cells instead of performing only one wash. To obtain the large CTL fraction, large TS32.15 CTLs were pelleted by centrifugation three times at 100 x g for 2 min, and non-pelleted small CTLs were removed after each centrifugation step.

When sorting for each of the three cell morphologies, 10 µl of cells from each collected fraction was immediately removed post sort for flow cytometry analysis. The remaining cells were then divided into three tubes to provide technical replicates. The cells were pelleted, the supernatant was removed by pipetting, and cell pellets were frozen at −80 °C until RNA extraction.

2.10. RNA sequencing

RNA library preparation, sequencing, and statistical analysis were performed by the USDA Warmwater Research Laboratory in Stoneville, MS. Total RNA was harvested from sorted cell pellets using the Lexogen Split RNA extraction kit. Samples were then run on TapeStation and only samples with eRIN greater than 8 were used in the analysis (Jeannotte et al., 2014). The libraries were constructed using the TruSeq Stranded mRNA kit (Illumina). Briefly, ~0.5 µg RNA was magnetically purified and fragmented using the kit reagents and cDNA synthesized with SuperScript II Reverse Transcriptase using random hexamer primers. cDNA was indexed through adaptor ligation to blunt ends, then further amplified by PCR using kit provided primers.

Analysis of the RNA-seq samples was done by mapping against reference genome GCA_001660625.1 for *Ictalurus punctatus* using hisat2 (Kim et al., 2017). To determine if additional genes not currently represented in the present genome existed, the de novo Trinity RNA-seq assembler was also used. Statistical analysis of differential expression of transcripts was performed using featureCounts and DESeq2 softwares (Haas et al., 2013; Liao et al., 2013; Love et al., 2014).

2.11. KEGG and gene ontology analysis

NCBI blastx of the transcripts were performed against the *Homo*

sapiens, *Ictalurus punctatus* and *Danio rerio* proteome from ENSEMBL in order to utilize the curated KEGG and gene ontology information (Kanehisa et al., 2016; Kersey et al., 2015). Due to *Ictalurus punctatus* not being annotated in any of the publicly available ontology database, the best blastx hit against the *Homo sapiens* was used to allow for analysis in the DAVID bioinformatics site (Huang et al., 2008).

2.12. Induction of apoptosis and TNP-specific IgM binding assays

To induce apoptosis, 1×10^6 cells/ml were washed three times in serum free media (AL-0) and incubated for 4 h or overnight with 2 mM DTT in AL-0 (Xiang et al., 2016). Cells were then washed three times to remove DTT. For assays examining binding of TNP-specific IgM, 5×10^6 cells were DTT treated, washed and resuspended in 500 µl catfish PBS, then divided in two aliquots. One cell aliquot was added dropwise to 1 ml cacodylate buffer (0.28 M cacodylic acid, 0.2 M NaCl, pH 6.9) supplemented with 4 mM picrylsulfonic acid, while the other cell fraction was added dropwise to 1 ml cacodylate buffer without picrylsulfonic acid. Tubes were gently rotated at 25 °C for 10 min protected from light, then washed with 1 ml catfish PBS. Washed cells were transferred to flow cytometry tubes and incubated on ice for 15 min with catfish RPMI/BSA, 20% heat inactivated catfish serum, or 0.15 µg/ml purified anti-TNP IgM. Cells were then stained for surface IgM with mAb 9E1 followed by goat anti-IgG_1:PE or goat anti-IgG_1:APC secondary antibody as described for flow cytometry. TNP-specific catfish IgM was affinity purified from the serum of a TNP:BSA-immunized catfish as described by van Ginkel et al. (1992).

2.13. Enzyme treatments

To determine the potential ligands for catfish natural IgM separate aliquots of 1×10^6 DTT treated apoptotic cells in AL-0 were incubated for 2 h at 28 °C without enzyme treatment (NT) or with one of the following treatments: 0.1 U/ml non-specific protease (protease type XIV, Streptomyces; Sigma), 10 U/ml DNase I (Ambion), 10 U/ml non-specific lipase (type II, porcine pancreas; Sigma), 10 U/ml PLA_2 (Sigma), 10 U/ml PLD (Sigma), 1 U/ml PLC (Sigma), or a mixture of glycosidases (25 U/ml N-glycanase, 6.25 U/ml O-glycanase, and 25 U/ml sialidase A; ProZyme). PLC and non-specific protease were used at 1 U/ml since the cells lost their integrity in pilot experiments with the higher concentration of 10 U/ml. Following the 2 h incubation, the enzyme was removed by washing the cells with catfish RPMI. Enzyme-treated and untreated cells were incubated in AL with or without 20% heat inactivated catfish serum for 15 min at 25 °C. Cells were then washed and stained with anti-catfish IgM mAb 9E1 followed by goat anti-mouse IgG_1:APC. To determine IgM binding in enzyme treated and untreated cells, the average median fluorescence intensities (MFI) were normalized based on the fluorescence with secondary (2°) Ab alone and compared to the normalized MFI of untreated cells according to the following formula:

$$\text{Normalized MFI} = \frac{(MFI_{serum}\,[enzyme\ treated] - MFI_{average\ 2°\ only}\,[enzyme\ treated])}{(MFI_{serum}\,[no\ treatment] - MFI_{average\ 2°\ only}\,[no\ treatment])} \times 100$$

2.14. Lipid binding assays

Possible lipid ligand(s) for catfish natural IgM were examined using the commercially available FlowPIPs multiplex lipid bead assay (Echelon). Lipid-conjugated beads were blocked with 1% BSA, then incubated with 1%, 5%, or 10% catfish serum diluted in blocking buffer (catfish PBS/1% BSA/0.09% N_3Na). The beads were then washed in blocking buffer including 0.05% Tween 20 and incubated with 50 µl blocking buffer containing 0.5 µg/ml anti-catfish IgM mAb 9E1 for 15 min on ice. Following incubation the beads were washed and incubated in 50 µl 0.005 µg/µl goat anti-mouse IgG_1:APC in blocking buffer. After the final wash, IgM:lipid interactions were analyzed by flow cytometry.

2.15. Clearance of IgM^+ CTLs by myelocyte enriched head kidney leukocytes

Catfish monocytes/macrophages were enriched from head kidney leukocytes as previously described (Booth et al., 2006). Briefly, one fish per experiment was sacrificed by tricaine overdose and pronephros (head kidney) tissue was passed through a 70 µm nylon filter (BD Falcon). The resulting cells were washed and resuspended in channel catfish macrophage medium (CCMM) consisting of RPMI Medium 1640 diluted 9:1 with H_2O and adjusted to contain 15 mM of Hepes Buffer, 0.18% sodium bicarbonate, 0.05 mM of 2-beta-mercaptoethanol and 5% heat-inactivated, pooled channel catfish serum. The head kidney leukocytes were plated at 1×10^7 cells/ml in poly-D-lysine coated 24 well plates. Cells were incubated for 24 h, and the wells were washed three times with sterile RPMI by gentle pipetting to remove non-adherent cells. Adherent cells were confirmed to be predominantly head kidney derived macrophages (HKDMs) by staining 3 wells with non-specific esterase (data not shown). Alternatively, macrophages from the catfish non-clonal 42 TA macrophage cell line, were enriched on poly-D-lysine coated plates as described above. TS32.15 CTLs were prepped by labeling with CellTrace Violet (Thermo Fisher Scientific) according to the manufacturer's directions, then cells were irradiated to prevent replication. Labeled and irradiated TS32.15 CTLs (2×10^6 cells/1 ml/well) were placed into wells with or without HKDMs, or 42 TA macrophages. The percentage of surface IgM^+ CTLs was monitored by staining for IgL-F and IgL-G chains and analyzing the CellTrace $Violet^+$ population (TS32.15 CTLs) at 24, 48 and 72 h.

3. Results

3.1. Clonal TS32.15 CTL exhibit functionally distinct morphologies

Clonal TS32.15 cells are not synchronized, and cultures consist of large elongated granular CTLs and smaller less granular CTLs. Microscopic examination of a TS32.15 culture when target 3B11 B targets are no longer present show small round cells ~10 µm in diameter and larger elongated cells that can extend to ~30 µm (Fig. 1A). Another important phenotypical distinction between the small and larger CTL morphologies is that only small CTLs can acquire serum IgM from the culture media, and these small cells stain positive with anti-catfish IgM 9E1 mAb. That these IgM positive cells are not residual target 3B11 B cells is supported by several lines of evidence. First, TS32.15 CTLs do not make RNA message for any of the catfish IgH or IgL chains (Fig. 1B). Second, even though the small CTLs stain positive for both IgL-F and IgL-G, which are the most prevalent IgL chains is catfish serum, isotypic exclusion has been demonstrated to occur in catfish B cells at both the protein and message levels. Third, 3B11 B cells express only IgL-F. Fourth, the small CTLs are negative for staining with mAb 3B6 (Fig. 1C). This mAb selectively binds only catfish 3B11 B cells and as such it can be used to monitor the presence of 3B11 stimulator/target cells in a culture and to exclude them from TS32.15 flow cytometry analysis. Also, 3B11 cells are typically cleared within 2–3 days after stimulation (see Fig. 1C, Supplemental Fig. 1, and Taylor et al., 2016). Scatter profiles of a typical TS32.15 culture at day 1 post stimulation (DPS) with irradiated 3B11 B cells and at 14 DPS is shown in Fig. 1D, and over time a clear shift to smaller and IgM^+ CTLs is observed, as defined by the S gate. That only small CTLs acquire IgM was also confirmed by dual staining with anti-catfish IgL-F and IgL-G (Fig. 1E).

In order to functionally define the different TS32.15 morphologies, CTLs within the S or L gates were enriched by FACS and the sorted cell populations were washed and examined for cytotoxic activity using ^{51}Cr-release assays. Sorted TS32.15 cultures with < 2% large CTLs did not lyse 3B11 targets, even at effector to target ratios of 5:1 (Fig. 1F), and reconstructed videos from stimulated TS32.15 cultures clearly demonstrate that only the larger “elongated” polymorphic TS32.15 CTLs

actively rearrange their cytoskeleton to sample their target cells (Supplemental Videos 1 and 2). Since the increase in the percentage of large TS32.15 CTLs routinely observed following stimulation can either be explained by increased replication of large CTLs and/or by small CTLs transitioning to large CTLs, small TS32.15 CTLs were FACS-sorted and membrane-labeled with Vybrant DiO. The labeled small CTLs were then recombined with unlabeled large TS32.15 CTLs and assayed by flow cytometry. By day 1 after recombination, the large CTLs had generally disappeared from the recombined cultures, however once the recombined cultures were restimulated with 3B11 target cells, large CTLs reappeared. Since these large CTLs fluoresced to a lesser degree than the originally labeled small CTLs, this finding provided evidence that small CTLs replicate and transition to large CTLs in response to stimulation (Supplemental Fig. 2). Also, here it should be noted that since labeling with Vibrant DiO did not result in a uniform membrane label, it was not possible to quantify the number of small CTL divisions.

3.2. Following stimulation small IgM$^-$ CTLs replicate and transition to larger CTLs, and large CTLs return to the smaller morphology and become IgM$^+$

To further understand the link between small IgM$^-$ CTLs, small IgM$^+$ CTLs, and large CTLs in response to stimulation, TS32.15 CTL cultures were stained with anti-catfish IgM mAb and the three populations (small IgM$^-$, small IgM$^+$, and large CTLs) were isolated by FACS. In addition, a fourth population containing both large and small IgM$^-$ cells was also obtained. All cell fractions were labeled with Cell Trace Violet, an amine binding dye that uniformly labels cells, to enable monitoring of cell division. Labeled CTLs were then placed in culture and stimulated with irradiated 3B11 targets. All sorted fractions exhibited substantial loss of larger CTLs after one day following sorting and stimulation (Fig. 2A and B). Large CTLs did not reappear in cultures of sorted fractions that initially contained high numbers of large CTLs (> 90%) or small IgM$^+$ CTLs (> 90%; see column 3 and 4). Sorts for small IgM$^-$ CTLs were performed on cultures that only contained a few large CTLs and these sorts yielded almost pure populations of IgM$^-$ CTLs (99%). However, post-sort cultures were repeatedly observed to be in the process of transitioning to the large CTL morphology, and this is likely due to their activation by the sorting procedure (Fig. 2B; column 2). Such cultures produced new large CTLs by 5 days post stimulation. In cultures sorted for both small and large IgM$^-$ TS32.15 CTLs (see column 1), a more robust recovery of large CTLs was observed as compared to cultures sorted for only small IgM$^-$ cells (column 2).

In addition to examining scatter profiles, the sorted and labeled cell fractions were also monitored for surface IgM throughout the time course, and this staining with mAb 9E1 demonstrated that some IgM$^-$ large CTLs became IgM$^+$ once they transitioned to the smaller morphology. Briefly, Cell Trace Violet staining of the four sorted cell populations demonstrated low replication levels in the culture sorted for small IgM$^+$ CTLs (Fig. 2C; right column) and this replication is entirely due to the small number of contaminating IgM$^-$ CTLs that were present from the beginning (Fig. 2C$_2$). The IgM$^+$ cells in this culture did not display any reduction in fluorescence indicative of cell replication. Similarly, large IgM$^-$ CTLs did not replicate (column 3). In cultures sorted for small IgM$^-$ CTLs, approximately 42% exhibited diminishing fluorescence, and there was an observed increase in large IgM$^-$ CTLs, indicating that transition from small to large was occurring. Consistent with this, all the cells in the L gate displayed reduced fluorescence (Fig. 2D). Similar results were obtained in cultures sorted for small and large IgM$^-$ CTLs, and here the small cells replicated more robustly during the 8 day time course (Fig. 2C and D; column 1). Importantly, large TS32.15 CTLs did not exhibit fluorescence intensities consistent with cell replication. Together these results provide evidence that only small IgM$^-$ CTLs replicate and transition to larger CTLs. To confirm that IgM$^+$ CTLs do not replicate, TS32.15 CTLs were subjected to cell cycle analysis. Briefly, cells were stained with anti-IgL-F and anti-IgL-G, fixed, permeabilized, treated with propidium iodide, and examined by flow cytometry. Gating on dual negative cells in the lower left quadrant showed DNA content reflective of all phases of the cell cycle. In contrast, dual IgL positive cells in the upper right quadrant were all in the G_0/G_1 phase (Fig. 2E).

Collectively, the data in Figs. 1 and 2 indicate that small IgM$^-$ TS32.15 CTLs replicate in response to stimulation and some transition to the large morphology. Large TS32.15 CTLs lyse targets, return to the small morphology, and stain positive for surface IgM. These IgM$^+$ TS32.15 CTLs do not replicate or change morphology after stimulation.

3.3. Catfish serum IgM binds early apoptotic T cells

Since IgM$^+$ TS32.15 CTLs did not replicate or shift to a cytotoxic morphology following stimulation with target cells, CTLs were stained for surface IgM, and incubated with annexin V and propidium iodide to determine if they were apoptotic. Assays were performed at 6, 8, and 14 days post stimulation. Briefly, on day 6 CTLs were predominantly non-apoptotic, and then over time they transitioned through an annexin V$^+$ IgM^{low} phase before the majority of CTLs became annexin V$^+$ IgM$^+$ (Fig. 3A). It should be noted, however, that most IgM$^+$ CTLs did not stain with propidium iodide indicating that IgM binds CTLs after phosphatidylserine is transferred to the outer leaflet of the plasma membrane, but prior to complete membrane permeabilization (Segawa and Nagata, 2015). Because human natural IgM is known to bind apoptotic T cells (Kim et al., 2002), it was speculated that catfish serum IgM may bind to other apoptotic cell including non-cytotoxic catfish T cells. To test this, two autonomous T cell lines (28S.3 and G14D; Miller et al., 1994a; Vallejo et al., 1991) were also examined for IgM binding. Catfish clonal T cell lines 28S.3 and G14D were originally cloned using limiting dilution from catfish PBL without stimulation. These clonal T cell lines are non-cytotoxic, and are akin to mammalian T helper cells. To induce apoptosis, the clonal T cells were treated with 2 mM DTT for 4 h, prior to staining with anti-catfish IgM, annexin V, and propidium iodide. Similar to the results observed with TS32.15 CTLs, apoptotic cells in both 28S.3 and G14D bound IgM. Even so, not all annexin V positive 28S.3 T cells are IgM$^+$, and these cells may also be transitioning through an annexin V positive, IgM$^-$ phase (Fig. 3B). In contrast to the clonal T cell lines, an MLC generated by stimulating PBLs from a non-immunized catfish with irradiated allogenic 3B11 B cells contained a small population of annexin V$^-$ IgM$^+$ cells. Since this population stained double positive for both IgL-F and IgL-G chains (data not shown), these cells likely represent NK cells armed with an ADCC-mediating FcμR described by Shen et al. (2003). Even so, after treatment with 2 mM DTT this MLC also exhibited an increase in both annexin V$^+$ and IgM$^+$ cells, which is reminiscent of a study that demonstrated that natural IgM binds lysophosphatidylcholine exposed on late apoptotic propidium iodide-positive Jurkat T cells (Kim et al., 2002).

To determine if catfish CTLs express an IgM-binding receptor or if natural IgM found in the catfish serum supplement in the culture media binds a ligand exposed on apoptotic CTLs, the following experiment was performed. Briefly, TNP-specific IgM was affinity purified from serum collected from a TNP:BSA-immunized catfish, and the ability of this TNP-specific IgM to bind apoptotic CTLs was examined. To expose potential IgM binding sites on TS32.15 CTLs, apoptosis was induced with 2 mM DTT under serum free conditions. One half of the apoptotic cells was haptenated with TNP and the other half was left untreated. To measure IgM binding, apoptotic TNP-haptenated and unhaptenated TS32.15 CTLs were incubated with 20% heat inactivated serum or TNP-specific IgM, then stained with anti-catfish IgM mAb. The CTLs were then analyzed by flow cytometry (Fig. 4A). Here, our results show that natural IgM from catfish serum binds unhaptenated apoptotic CTLs, while TNP-specific IgM did not bind unhaptenated apoptotic CTLs. Thus, we believe this experiment provides strong evidence that IgM binding to apoptotic CTLs occurs through specific recognition via the Fab region, and is not mediated by an FcμR.

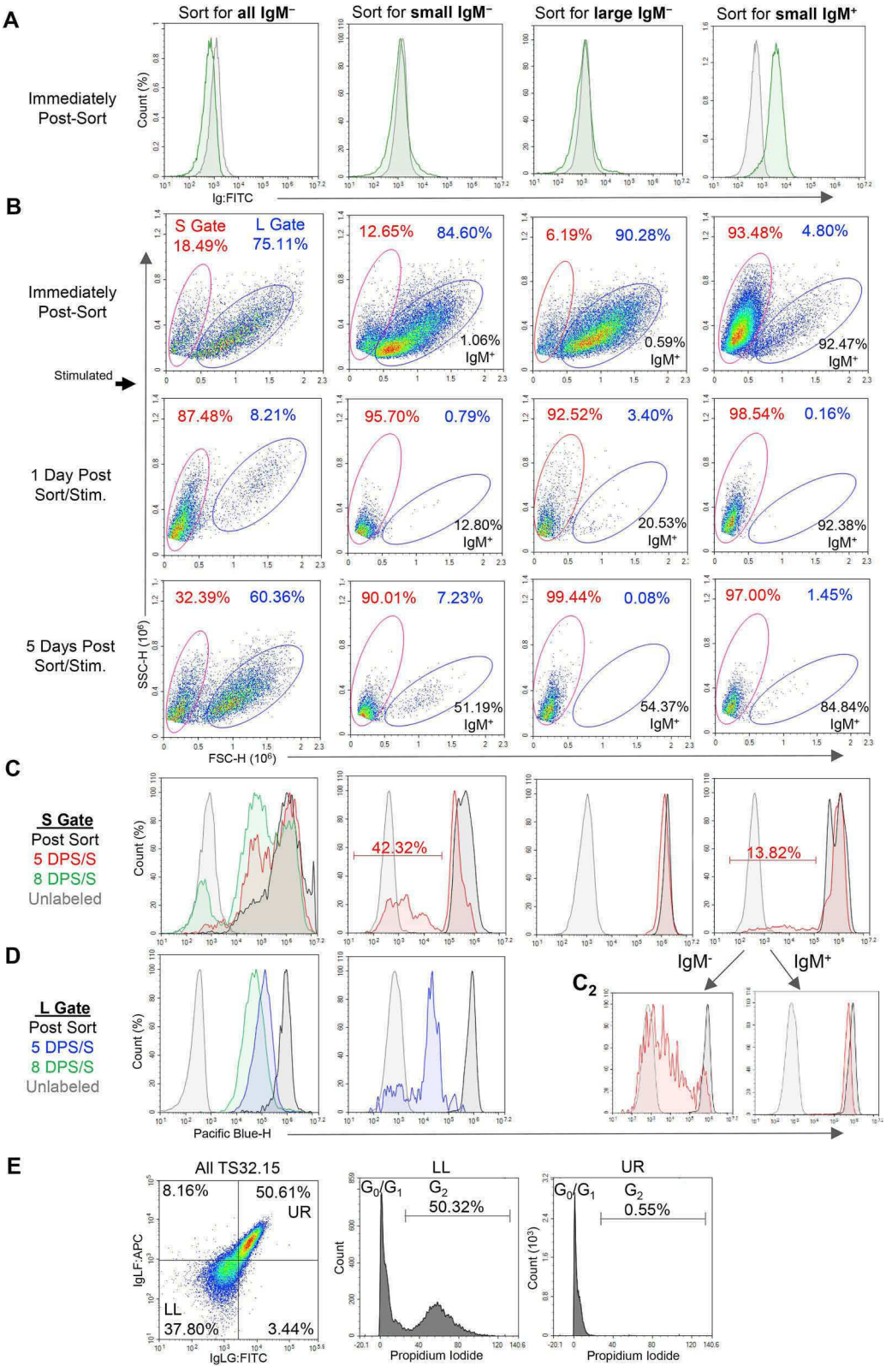

Fig. 2. Small IgM⁻ TS32.15 CTLs replicate and transition to a larger morphology following stimulation, while large TS32.15 CTLs become small and are not reactivated. TS32.15 CTLs were stained with anti-catfish IgM mAb 9E1 followed by goat anti-mouse IgG_1:FITC, then FACS sorted for size and fluorescence (IgM^+ or IgM^-) as indicated by the header of each column. Sorted CTLs were immediately membrane-labeled with CellTrace Violet and stimulated with irradiated 3B11 target cells, then cultured in triplicate and monitored for size, IgM binding, and cell division. Data is representative of triplicate measurements and of two independent experiments. Note that the headers for each column apply to panels A–D. **(A)** Histograms of IgM:FITC (green) on CTLs immediately post sorting. Staining with anti-rainbow trout IgM (grey) is shown as an isotype control. **(B)** Scatter profile density plots of sorted CTLs immediately, 1 day, and 5 days post sorting and stimulation are presented; percentage of IgM^+ CTLs within the S gate is also indicated. 3B11 target cells were excluding from the analysis using mAb 3B6. **(C)** Division of TS32.15 CTLs in the S gate is visualized by normalized fluorescence histograms. Overlays of the sorted and labeled CTLs are provided for immediately (black lines), 5 days (red histograms) and 8 days (green, where applicable) after sorting and stimulation. Unlabeled CTLs are provided as a baseline control (grey). **(C_2)** Normalized fluorescence histograms of the culture are shown in column 4 at 5 days post stimulation and are gated on IgM^- and IgM^+ small cells. **(D)** Normalized fluorescence histograms of TS32.15 CTLs in the L gate immediately (black), 5 days (red), and 8 days (green, where applicable) after sorting and stimulation. Unlabeled TS32.15 CTLs are provided as a baseline control (grey). **(E)** TS32.15 CTLs were dual stained for catfish IgL-F and IgL-G using mAbs 3F12 and 11A2 followed by goat anti-mouse IgG_1:APC and IgG_{2b}:FITC respectively, then fixed with formaldehyde and permeabilized with methanol. The genomic DNA in the fixed and permeabilized cells was then stained with propidium iodide. Cell cycle plots depict propidium iodide staining for the IgL^- and IgL^+ CTLs. Data is representative of 3 independent MLC cultures. (For interpretation of the references to colour in this figure legend, the reader is referred to the Web version of this article.)

3.4. Catfish natural IgM binds PIP_2 on apoptotic CTLs

To determine potential ligands for catfish natural IgM, apoptotic TS32.15 CTLs were treated separately with either a glycosylase mixture, DNase I, non-specific lipase, phopholipase C (PLC), phospholipase D (PLD), phospholipase A_2 (PLA_2), or a non-specific protease mixture, for 2 h. Following the enzymatic treatments, the CTLs were incubated with 20% heat inactivated catfish serum, and IgM-binding was measured by flow cytometry (Fig. 4B). Treating CTLs with lipase, and more specifically with PLC or PLD, reduced IgM-binding. While these enzyme

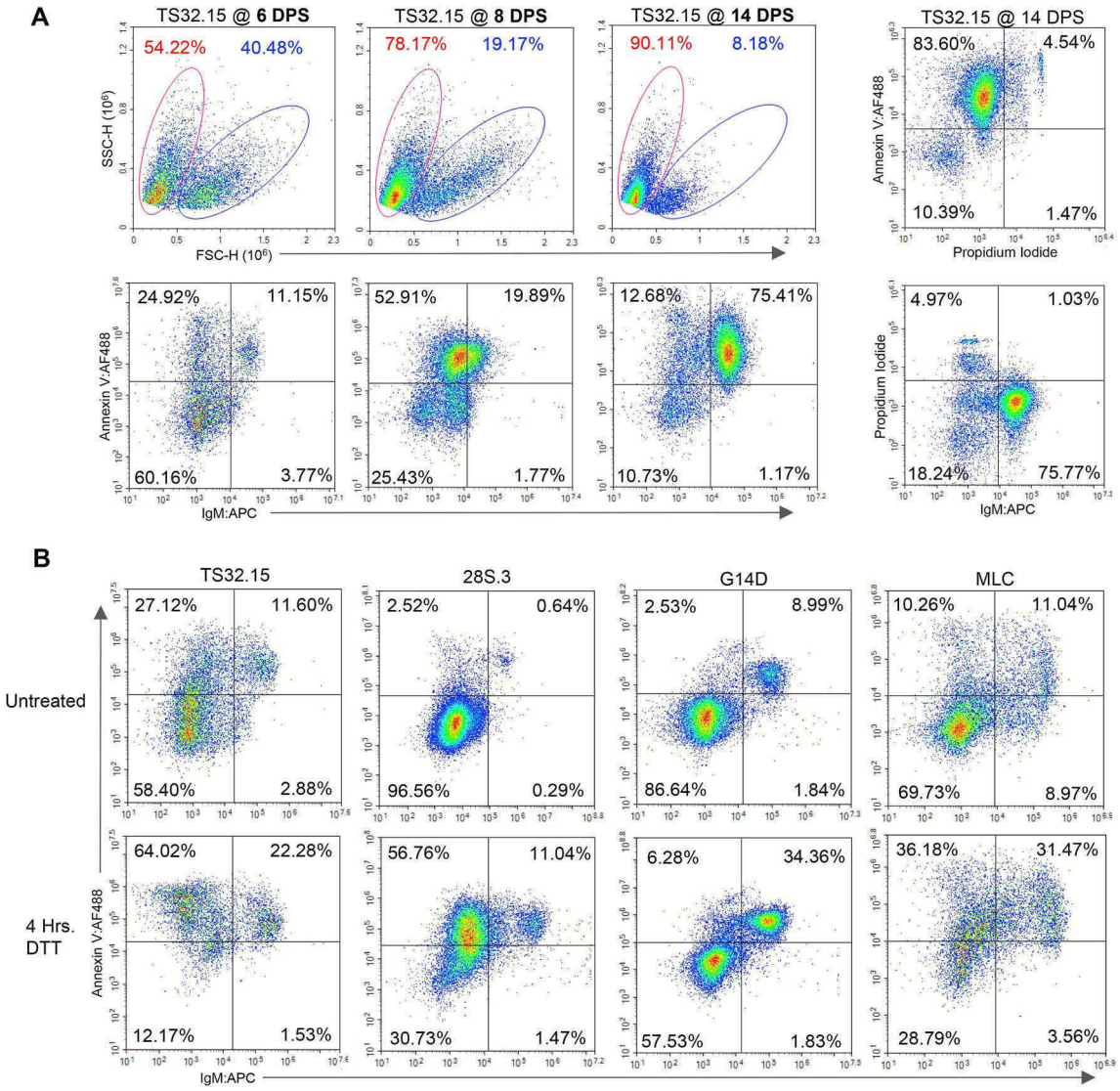

Fig. 3. IgM$^+$ TS32.15 CTLs are early apoptotic. (A) CTLs from a TS32.15 culture were stained with anti-catfish IgM mAb 9E1 followed by goat anti-mouse IgG1:APC at 6, 8, and 14 days post stimulation (DPS) to detect surface IgM binding. Afterwards the CTL were washed and immediately treated with propidium iodide and annexin V conjugated to Alexa Flour 488. At 14 DPS, the majority of IgM$^+$ TS32.15 CTLs bind Annexin V but do not stain with propidium iodide. **(B)** IgM binds catfish apoptotic clonal non-cytotoxic T cells 28S.3 and G14D, and apoptotic cells in MLCs. TS32.15 CTLs, 28S.3 T cells, G14D T cells, and catfish MLCs were incubated in catfish AL-4 media containing 2 mM DTT to induce apoptosis or in catfish AL-4 without DTT. Following incubation, the cells were stained for surface IgM using anti-catfish IgM mAb 9E1 followed by goat anti-mouse IgG1:APC. The cells were then stained with propidium iodide and annexin V conjugated to Alexa Flour 488. MLC data is representative of 3 independent MLCs each from a different catfish.

treatments reduced IgM-binding, treatment with proteases, however consistently resulted in higher levels of bound IgM, and this finding may be due to the depletion of surface proteins that interfered with IgM ligand accessibility. Also, since one of the predominant targets of mammalian natural IgM is phosphorylcholine (Gronwall et al., 2012; Holodick et al., 2017), we tested the ability of catfish serum IgM to bind the *Haemophilus influenzae* strain Δrep rcp5, which is engineered to constitutively express phosphorylcholine, and IgM binding was not observed (data not shown). In order to examine other potential lipid ligands, we took advantage of a commercially available multiplex phospholipid bead assay that allowed us to examine binding of 11 specific phospolipids. Using this multiplex assay, catfish IgM was found to bind phosphatidylinositol 4,5-bisphosphate (PIP_2; Fig. 4C).

Taken together, this result and the finding that treatment with PLC and PLD also reduce catfish IgM binding to apoptotic TS32.15 CTLs demonstrate that natural IgM in catfish binds lipids, including PIP_2 exposed on catfish apoptotic T cells.

3.5. Small IgM$^+$ TS32.15 CTLs are efficiently cleared by macrophages

In mammals, macrophages recognize and clear apoptotic cells prior to these cells undergoing secondary necrosis and release of intracellular components that can induce inflammation (Hesketh et al., 2015; Toda et al., 2015). To test if apoptotic IgM$^+$ CTLs are cleared by catfish macrophages, catfish HKDMs were obtained by plating head kidney leukocytes on lysine coated plates and after 24 h incubation, the plates were washed three times to remove non-adherent cells (Booth et al., 2006). The TS32.15 CTLs labeled with CellTrace Violet, were irradiated to prevent their replication, incubated with the adherent macrophages and examined by flow cytometry at 24, 48 and 72 h. This labeling of TS32.15 CTLs with CellTrace Violet as defined by gate 1 allowed us to track the small CTLs within the S gate as IgM$^+$, based on their dual staining for both IgL-F and IgL-G during this timeframe (Fig. 5A). After 24 h of incubation without macrophages, high levels of small IgM$^+$ CTLs remained (~90%), however the numbers of small IgM$^+$ CTLs were substantially reduced in cultures incubated with HKDM. The percentage

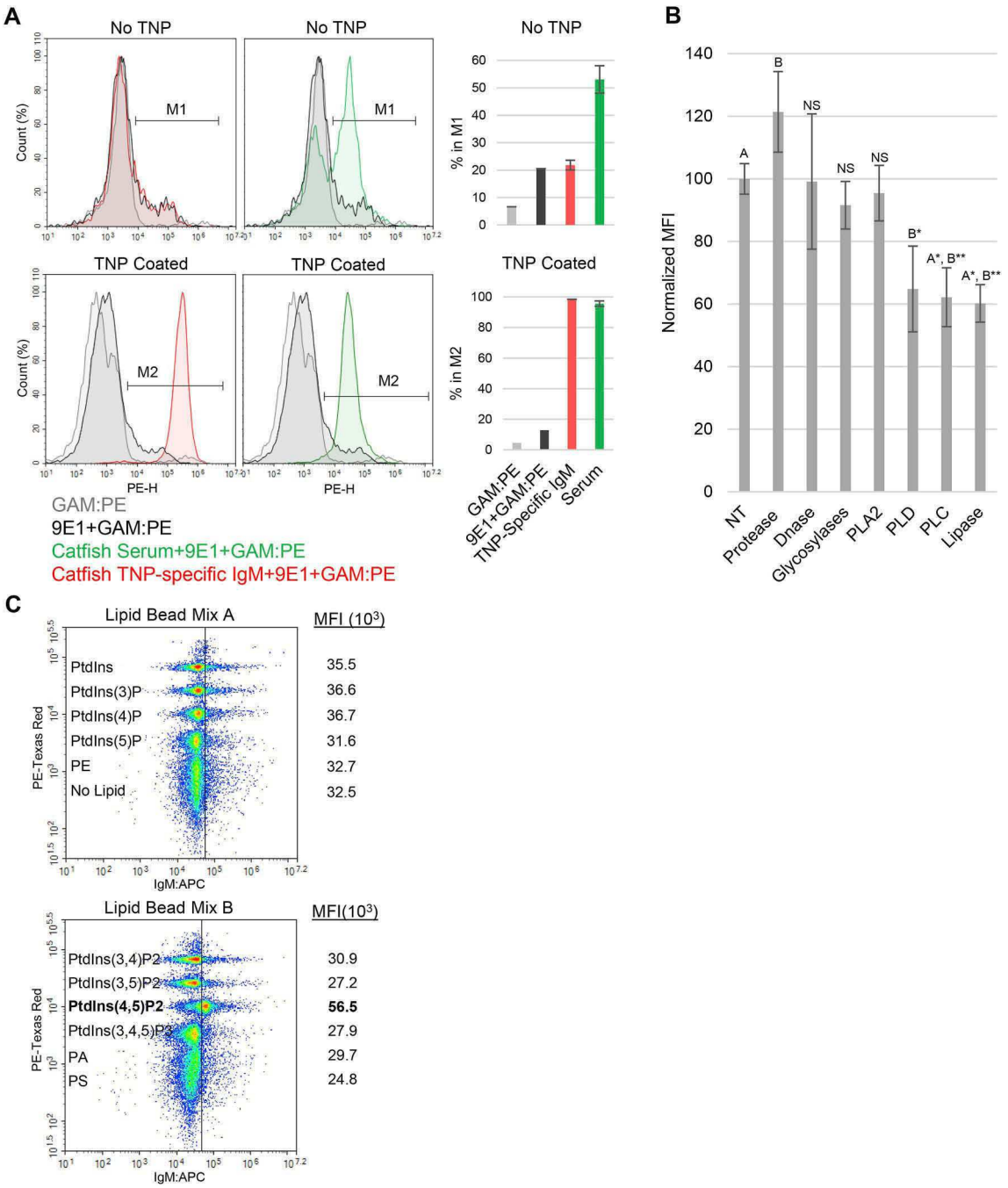

Fig. 4. Natural IgM acquired from the catfish serum in the culture media binds inositol lipid PtdIns(4,5)P2) on apoptotic IgM$^+$ TS32.15 CTLs. (A) 5×10^6 TS32.15 CTLs were incubated overnight with 2 mM DTT to induce apoptosis, the cells were then washed in catfish PBS and divided equally into two aliquots. The CTLs in one aliquot were TNP-haptenated. The TNP-haptened and unhaptenated CTLs were incubated with 20% catfish serum or TNP-specific IgM for 15 min on ice, washed and then stained with anti-catfish IgM 9E1 followed by goat anti-mouse IgG1:PE (GAM). The average percentage of cells in the M1 and M2 gates of two technical replicates, +/− the standard error, is shown at right. Data is representative of three independent experiments. **(B)** Alternatively, the apoptotic TS32.15 CTLs were treated with a mixture of non-specific proteases, DNAase I, a mixture of glycosylases, PLA_2, PLD, PLC, or non-specific Lipase, for 2 h. The enzyme treated CTLs were then washed and incubated in AL-4 supplemented with 20% catfish serum. IgM-binding was analyzed by flow cytometry and the median fluorescence intensities (MFIs) were normalized to that of the untreated samples (NT = 100%) as described in the methods, and the average MFI ± the standard error is shown. A one way ANOVA followed by Tukey HSD significance was performed, and groups with the same letters are significant; n = 6, *p < 0.05, **p < 0.01. Data is compiled from two (DNase I, PLA_2, PLD, and PLC) or three (all others) independent experiments. **(C)** A representative Multiplex Lipid Beads (Echelon) panel is shown where beads were incubated with 10% catfish serum diluted in blocking buffer and then stained with anti-catfish IgM mAb 9E1 followed by goat anti-mouse IgG_1:APC. The MFI of IgM staining for each lipid is indicated; PtdIns (phosphatidylinositol), PE (Ptdenthanolamine), PA (phosphatidic acid), PS (phosphatidylserine).

of small IgM$^+$ TS32.15 CTLs decreased even further after 48 h of co-incubation with HKDM (Fig. 5B), and at 72 h very few small IgM$^+$ CTLs remained (data not shown). This was consistent in all three experimental replicates. Similar results were also observed in an additional experiment performed with the catfish macrophage cell line 42 TA (data not shown).

3.6. TS32.15 CTL transcriptome analyses

To determine if the observed CTL populations represent distinct differentiation stages, transcriptome sequencing of RNA from sorted memory-like small IgM$^-$ cells, large cytotoxic effector cells, and small

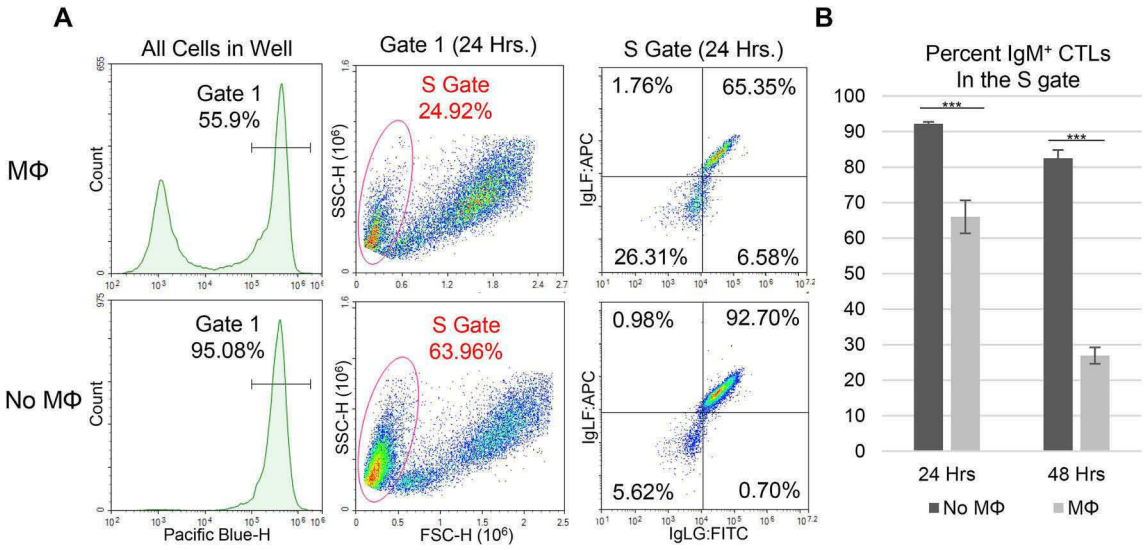

Fig. 5. IgM$^+$ TS32.15 CTLs are preferentially cleared by macrophages. TS32.15 CTLs were labeled with CellTrace Violet, irradiated and incubated with catfish head kidney derived macrophages (MΦ) defined as the adherent population of head kidney leukocytes. **(A)** The percentages of IgM$^+$ CTLs were determined by staining with anti-catfish IgL-F 3F12 followed by goat anti-mouse IgG1:APC and anti-catfish IgL-G mAb 11A2 followed by goat anti-mouse IgG2b:FITC. Cell percentages are indicated in each quadrant. The gating strategy from a representative experiment at 24 h after co-incubation with or without MΦ; cells positive for CellTrace Violet were further gated on small cells and examined for the presence of dual IgL chain positive cells. This strategy was used to obtain the data presented in panel B. **(B)** Percent IgM$^+$ CTLs found within the S gate at 24 and 48 h after incubation. Very few small TS32.15 CTLs were found at 72 h. The data is representative of 3 independent experiments. N = 6, ** = p value < 0.01, *** = p value < 0.001. (For interpretation of the references to colour in this figure legend, the reader is referred to the Web version of this article.)

IgM$^+$ apoptotic cells was performed. However, there are classical caveats of RNA-seq analysis in non-model organisms which should be kept in mind 1) as stated in the methods, the annotation was performed against the human database to enable the use of KEGG's tools 2) many species specific genes remain uncharacterized to this date, and 3) members of multigene families likely are not represented correctly due to mapping difficulties and elimination of all reads mapping at more than one location. Even so, we believe our transcriptome studies yielded some interesting information as summarized below. Examples of transcripts with differential expression is presented in Supplemental Table 2.

3.6.1. Small IgM$^-$ cell transcripts

- Transcripts with significantly higher expression in small IgM$^-$ cells as compared to both the large effector cells and small IgM$^+$ cells included: macrophage mannose receptor 1, interleukin-12β, transcription factor SOX-6 and an HSP70 family member. Several other transcripts encoding heat shock proteins were also overexpressed when small IgM$^-$ and small IgM$^+$ cells were compared.
- Transcripts with significantly higher expression in small IgM$^-$ cells as compared to effector cells included transcripts for TNF-α, perforin, and actin.
- Transcripts encoding proteins associated with TNF receptor signaling, the PI3K-Akt signaling pathway and antigen processing and presentation, were enriched in small IgM$^-$ cells as compared to large effector cells.
- Transcripts encoding telomerase reverse transcriptase and regulator of telomere elongation helicase, DNA replication factors, several DNA polymerase subunits, and proliferating cell nuclear antigen were significantly upregulated in the small IgM$^-$ cells as compared to the large CTLs.
- Transcripts for cyclins and cyclin dependent kinases were expressed at a significantly higher level in small IgM$^-$ cells as compared to the large CTLs.

3.6.2. Large effector CTL transcripts

- Transcripts for caveolin-2-like and nuclear factor of activated T-cells, cytoplasmic 2 (NFATc2) were significantly upregulated in large effector cells as compared to both IgM$^-$ and IgM$^+$ small cells.
- In comparison with small IgM$^-$ cells, large effector CTLs expressed higher levels of transcripts that encode actin-related protein 2A, CD2-associated protein and talin-2.
- Transcripts for cytokine receptors, (IL-17RE, IL-7RA, IL-11RA), chemokines, chemokine receptors and proteins involved in signaling were upregulated as compared to small IgM$^-$ cells.
- In comparison to small IgM$^+$ cells, large effector cells expressed transcripts encoding TGF-β receptor type-1 and interleukin-2 receptor subunit β at significantly higher levels.
- Lysosome-associated membrane glycoprotein 1 (LAMP1, CD107a) transcripts were significantly upregulated in large effector cells as compared to small IgM$^+$ cells.
- Several transcription factors including Krueppel-like factor 7, NFATc1, bcl6, and AP1 were upregulated in large effector cells as compared to small IgM$^+$ cells.
- Transcripts for the pro-apoptotic protein, Bax, were upregulated, while gene expression of p53, bcl-2, and several cell cycle regulators were downregulated.

3.6.3. Small IgM$^+$ cell transcripts

- Transcripts for the Sphingosine1-phosphate receptor 4 (S1PR4) were highly enriched in small IgM$^+$ cells as compared to both small IgM$^-$ cells and large effector cells.
- Small IgM$^+$ cells as compared to large effector cells expressed higher levels of IL-34, TNF-α and CXCL8.
- Transcripts for the initiator caspase-8 and the executioner caspase-3 were upregulated in small IgM$^+$ cells as compared to large effector cells.
- Transcripts for NK-lysins were upregulated in small IgM$^+$ cells in comparison with small IgM$^-$ cells.
- Transcripts for enzymes involved with carbohydrate metabolism

were also upregulated in small IgM$^+$ cells when compared to small IgM$^-$ cells.

4. Discussion

Over the years, studies of T cell differentiation in mammalian models have often resulted in conflicting findings and several models have been proposed for the order in which effector and memory cells develop. In addition, how differences in antigen signal strength, co-stimulation, and cytokines at the time of activation impact the differentiation fate have also been considered. As a consequence, the classification of each subset has over time been redefined and through this process well-defined markers are now used to identify multiple T cell effector and memory subsets (Chang et al., 2014; Herndler-Brandstetter et al., 2018; Patil et al., 2018). For example, for CD8 T cell subsets, short lived effector T cells can be CD127$^-$ (IL7Rα)$^-$, KLRG1$^+$, CD8$^+$ and they express high levels of granzymes, while memory precursor effector T cells can be classified as CD127$^+$, KLRG1$^-$, IL-2 producing CD8$^+$ T cells. Central memory CD8$^+$ cells can be classified as CD62L$^+$, CD127$^+$, while effector memory cells are defined as CD62L$^-$, CD127$^+$. Furthermore, the ability of memory T cells to self-renew is due to their defining transcription factor T cell factor 1 (Tcf1; encoded by the Tcf7 gene). In comparison, while a faster and longer lasting immune response to *Ictalurid herpesvirus-1* (channel catfish virus) after booster immunization provides evidence for the existence of memory CTLs in catfish (Taylor et al., 2016), markers such as KLRG1 and L-selectin have not been identified. Nevertheless, while it is difficult to classify the TS32.15 cell line, our findings presented here demonstrate that catfish clonal TS32.15 CTLs expanded by alloantigen stimulation are heterogeneous in their morphology, immediate function, and are represented by three differentiation stages: 1) small memory-like CTLs, 2) terminally differentiated effector CTLs, and 3) small IgM$^+$ senescent CTLs. The small IgM$^-$ CTLs replicate in response to stimulation with specific antigen, i.e. 3B11 B cells, and this replication maintains the pool of CTLs that retain their ability to respond when re-exposed to their specific antigen. These memory cells express message for perforin and TNF-α, and some transition into the morphologically larger, elongated CTLs that readily lyse targets. The large effector cells express message for the memory marker CD127$^+$ and actively sample their environment. After killing their targets, or in the prolonged absence of stimulation, these larger effector CTLs, shift to the smaller round morphology. These small CTLs can no longer become activated, do not proliferate, and become apoptotic and stain positive for natural IgM, which is acquired from the culture media (see Fig. 3).

In mammals, the binding of natural IgM to apoptotic T cells has been shown to aid in their clearance by macrophages (Gronwall et al., 2012). For example, using human peripheral blood T cells and Jurkat cells, Kim et al. (2002), demonstrated that natural IgM from human normal serum binds late apoptotic T cells that stain with annexin V and propidium iodide. This IgM binding also enhanced C1q binding to the apoptotic cells, and the authors determined that the binding was via the Fab fragment of IgM, and not its Fc portion. Notably, the IgM binding was enhanced after cells were treated with PLA_2, an enzyme that catalyzes the hydrolysis of plasma membrane phospholipids which results in the release of arachidonic acid and lysophospholipids. In addition, IgM binding was also decreased when cells were treated with PLD, which cleaves the polar head groups of lysophospholipids. To confirm that natural IgM antibodies recognize lysophosphatidylcholine and the phosphocholine head groups, the authors also used a plate absorption assay. In comparison, catfish natural IgM was shown to bind the head group of phosphatidylinositol bisphosphate (PIP_2) on early apoptotic CTLs (annexin V$^+$, PI$^-$). In this regard however, it is important to emphasize that only 11 phospholipids were included in the Echelon bead assay and it seems likely that other natural IgM antibodies in catfish serum could target different membrane lipids. For example, one candidate would be cardiolipin, which is normally confined to mitochondrial membranes, has also been shown to be expressed in surface blebs on early apoptotic mammalian cell lines (Manganelli et al., 2015; Sorice et al., 2000). Also, even though catfish natural IgM did not bind the phosphorylcholine expressing *H. influenzae* strain Δrep rcp5, we cannot exclude that oxidation-specific epitopes of phosphatidylcholines could be recognized (Gronwall et al., 2012). In addition, studies have demonstrated that fish natural IgM can bind other cellular targets such as single-stranded DNA, thyroglobulin and actin (Gonzalez et al., 1988). While the finding that catfish head kidney derived HKDMs can effectively clear IgM$^+$ apoptotic cells within 48 h is not surprising, it does suggest an *in vivo* role for this specific natural IgM. For example, this antibody may mediate phagocytosis indirectly through recruitment of complement components, or it could be recognized by macrophages via their expression of a yet unidentified phagocytic FcμR, similar to the Fc receptor FCMR reviewed in Wang et al. (2016). It is also possible, that other macrophage PRRs, e.g. scavenger receptors, if they bound phosphatidyl serine directly could be involved and aid in the clearance of apoptotic cells. Thus, by staining cells with anti-IgM and annexin V, it becomes possible to discriminate between FcμR bearing cells and senescent cells.

Even though our transcriptome analyses are preliminary, they do provide some clarification on the proposed three differentiation stages 1) small memory-like CTLs, 2) terminally differentiated effector CTLs, and 3) small IgM$^+$ senescent CTLs. Briefly, our data validated the finding that only small IgM$^-$ cells replicate and large effector cells do not since transcripts encoding DNA replication factors, DNA polymerase subunits and cell cycle regulators were significantly upregulated in the small IgM$^-$ cells as compared to the large CTLs. Also, transcripts for proteins involved with the elongation and protection of telomeres during DNA replication were more abundant in small IgM$^-$ cells as compared to large cells. This finding is in agreement with results from our previous studies demonstrating that transient telomerase activity is induced in TS32.15 CTLs after each round of stimulation with 3B11 targets (Barker et al., 2002; Barker, 2001). Maintaining telomere length is likely important for the long term self-renewal of the pool of small-memory like cells, and that TS32.15 CTLs exhibit short but stable telomeres similar to the catfish autonomous clonal cell lines was previously shown using the telomere restriction fragment (TRF) assay (Barker, 2001). In addition, that transcripts for perforin, TNF-α and actin were upregulated in small IgM$^-$ cells as compared to large CTLs, indicate that these cells are transitioning to effector cells.

Large TS32.15 CTLs expressed significantly higher levels of multiple transcripts that reflected their effector function. For example, caveolin-2 transcripts were expressed at higher levels compared to both IgM$^-$ and IgM$^+$ small cells and this may be an important finding. Caveolins are the main protein components of caveolae present in lipid rafts of the plasma membrane and caveolae function both in protein trafficking and signal transduction (Lajoie and Nabi, 2010; Gonçalves de Almeida, 2017). Similarly, as compared to small IgM$^-$ cells, transcripts for proteins that are directly involved with actin remodeling and membrane trafficking (CD2-associated protein, talin-2) were upregulated, and this is consistent with the observed higher mobility of catfish large CTL effectors (Spencer, 2018). Compared to the small IgM$^+$ cells, large effector cells expressed increased levels of transcripts for proteins that are involved with IL-2 signaling (IL-2RB, STAT5B, calcineurin, NFAT and AP1). Here, it is also important to emphasize that TS32.15 CTLs require the addition of exogenous growth factors included in the culture media for long term survival. These growth factors are provided in the form of a culture supernatant from catfish clonal 28S T cells, and likely includes IL-2 (Wilson et al., 1998b). That transcripts for cell cycle regulators were downregulated, while *BAX* expression was upregulated, also support the large CTLs as terminal effectors.

In agreement with the observation that small IgM$^+$ cells are apoptotic, transcripts for the initiator caspase-8 and the executioner caspase-3 were upregulated. Interestingly these cells express transcripts for IL-34 and inflammatory cytokines, TNF-α and CXCL8. Moreover, secretion

of inflammatory cytokines is not a hallmark of apoptotic cells, instead inflammatory cytokines are known to be secreted by senescent cells and as such they contribute to the so-called senescence-associated secretory phenotype (SASP; Coppé et al., 2010). Nevertheless, these cytokines are involved in macrophage activation and neutrophil recruitment which aids in the clearing of small IgM^+ cells. The high expression of sphingosine1-phosphate receptor 4 (S1PR4) transcripts in small IgM^+ cells as compared to both small IgM^- cells and large effector cells is also interesting. S1PR4 belongs to a group of five different G-protein coupled receptors and while S1PR1, 3, and 5 have been shown to regulate T cell chemotaxis (Dorsam et al., 2003). Recently, it was shown in mice that naive T cells are chemoattracted by S1Ps while effector and memory T cells do not migrate toward S1Ps, and that the ratio between S1PR1 and S1PR2 controls the migration (Drouillard et al., 2018). Whether the catfish S1PR4 transcript encodes a protein that regulates chemotaxis in catfish remains to be determined. Unexpectedly, transcripts for NK-lysins were also upregulated in small IgM^+ cells as compared to large effector cells and the significance of this is unknown. Although it may be that catfish NK-lysins are involved in autophagy, which was recently shown for Turbot NK-lysin in erythrocytes (Pereiro et al., 2017).

In summary, this study presents a first assessment of CTL dynamics in a teleost fish model and it emphasizes the utility of the catfish TS32.15 CTL line. However, whether the small IgM^+ cells that are recognized by natural IgM are truly senescent or early apoptotic is still debatable. The data presented here provide a framework to design future more targeted studies to examine how CTL subsets are regulated in fish.

Acknowledgements

This work was supported by U.S. Department of Agriculture-National Institute of Food and Agriculture Predoctoral Fellowship 2017-67011-26047 to (to D.A.S) and the National Science Foundation Grant IOS-1655419.

All FACS experiments were performed at the UMMC Cancer Institute Flow Cytometry Core Facility, which is supported in part through the UMMC Mississippi Center of Excellence in Perinatal Research (MS-CEPR)-COBRE (P20GM121334\).

We thank Drs. Brian Akerley and Sandy Wong for providing the *Haemophilus influenzae* strain Δrep rcp5.

Appendix A. Supplementary data

Supplementary data to this article can be found online at https://doi.org/10.1016/j.dci.2018.11.001.

References

Barker, K., Khayat, M., Miller, N., Wilson, M., Clem, L.W., Bengten, E., 2002. Immortal and mortal clonal lymphocyte lines from channel catfish: comparison of telomere length, telomerase activity, tumor suppressor and heat shock protein expression. Dev. Comp. Immunol. 26, 45–51.

Barker, K.S., 2001. Analysis of Factors that May Be Involved in the Immortalization of Leukocytes from the Channel Catfish (Ictalurus punctatus), Microbiology and Immunology. University of Mississippi Medical Center 2500 North State Street Jackson MS 39216.

Booth, N.J., Elkamel, A., Thune, R.L., 2006. Intracellular replication of Edwardsiella ictaluri in channel catfish macrophages. J. Aquat. Anim. Health 18, 101–108.

Chang, J.T., Wherry, E.J., Goldrath, A.W., 2014. Molecular regulation of effector and memory T cell differentiation. Nat. Immunol. 15, 1104–1115.

Coppé, J.-P., Desprez, P.-Y., Krtolica, A., Campisi, J., 2010. The senescence-associated secretory phenotype: the dark side of tumor suppression. Annual Review of Pathology 5, 99–118.

Cornish, G.H., Sinclair, L.V., Cantrell, D.A., 2006. Differential regulation of T-cell growth by IL-2 and IL-15. Blood 108, 600–608.

Deluca, D., Wilson, M., Warr, G.W., 1983. Lymphocyte heterogeneity in the trout,Salmo gairdneri, defined with monoclonal antibodies to IgM. Eur. J. Immunol. 13, 546–551.

Dorsam, G., Graeler, M.H., Seroogy, C., Kong, Y., Voice, J.K., Goetzl, E.J., 2003. Transduction of multiple effects of sphingosine 1-phosphate (S1P) on T cell functions by the S1P1 G protein-coupled receptor. J. Immunol. 171, 3500–3507.

Drouillard, A., Neyra, A., Mathieu, A.L., Marcais, A., Wencker, M., Marvel, J., Belot, A., Walzer, T., 2018. Human naive and memory T cells display opposite migratory responses to sphingosine-1 phosphate. J. Immunol. 200, 551–557.

Edholm, E.S., Stafford, J.L., Quiniou, S.M., Waldbieser, G., Miller, N.W., Bengten, E., Wilson, M., 2007. Channel catfish, Ictalurus punctatus, CD4-like molecules. Dev. Comp. Immunol. 31, 172–187.

Gonçalves de Almeida, C.J., 2017. Caveolin-1 and caveolin-2 can Be antagonistic partners in inflammation and beyond. Front. Immunol. 8, 1530.

Gonzalez, R., Charlemagne, J., Mahana, W., Avrameas, S., 1988. Specificity of natural serum antibodies present in phylogenetically distinct fish species. Immunology 63, 31–36.

Gronwall, C., Vas, J., Silverman, G.J., 2012. Protective roles of natural IgM antibodies. Front. Immunol. 3, 66.

Haas, B.J., Papanicolaou, A., Yassour, M., Grabherr, M., Blood, P.D., Bowden, J., Couger, M.B., Eccles, D., Li, B., Lieber, M., 2013. De novo transcript sequence reconstruction from RNA-seq using the Trinity platform for reference generation and analysis. Nat. Protoc. 8, 1494–1512.

Herndler-Brandstetter, D., Ishigame, H., Shinnakasu, R., Plajer, V., Stecher, C., Zhao, J., Lietzenmayer, M., Kroehling, L., Takumi, A., Kometani, K., Inoue, T., Kluger, Y., Kaech, S.M., Kurosaki, T., Okada, T., Flavell, R.A., 2018. KLRG1(+) effector CD8(+) T cells lose KLRG1, differentiate into all memory T cell lineages, and convey enhanced protective immunity. Immunity 48, 716–729.

Hesketh, E.E., Dransfield, I., Kluth, D.C., Hughes, J., 2015. Circulating IgM requires plasma membrane disruption to bind apoptotic and non-apoptotic nucleated cells and erythrocytes. PloS One 10, e0131849.

Hogan, R.J., Waldbieser, G.C., Goudie, C.A., Antao, A., Godwin, U.B., Wilson, M.R., Miller, N.W., Clem, L.W., McConnell, T.J., Wolters, W.R., Chinchar, V.G., 1999. Molecular and immunologic characterization of gynogenetic channel catfish (Ictalurus punctatus). Mar. Biotechnol. 1, 317–327.

Holodick, N.E., Rodriguez-Zhurbenko, N., Hernandez, A.M., 2017. Defining natural antibodies. Front. Immunol. 8, 872.

Huang, D.W., Sherman, B.T., Lempicki, R.A., 2008. Systematic and integrative analysis of large gene lists using DAVID bioinformatics resources. Nat. Protoc. 4, 44.

Jeannotte, R., Lee, E., Kong, N., Ng, W., Kelly, L., Weimer, B., 2014. High-throughput Analysis of Foodborne Bacterial Genomic DNA Using Agilent 2200 TapeStation and Genomic DNA ScreenTape System. Agilent Technologies.

Kanehisa, M., Sato, Y., Kawashima, M., Furumichi, M., Tanabe, M., 2016. KEGG as a reference resource for gene and protein annotation. Nucleic Acids Res. 44, D457–D462.

Kersey, P.J., Allen, J.E., Armean, I., Boddu, S., Bolt, B.J., Carvalho-Silva, D., Christensen, M., Davis, P., Falin, L.J., Grabmueller, C., 2015. Ensembl Genomes 2016: more genomes, more complexity. Nucleic Acids Res. 44, D574–D580.

Kim, D., Langmead, B., Salzberg, S., 2017. HISAT2: Graph-based Alignment of Next-generation Sequencing Reads to a Population of Genomes.

Kim, S.J., Gershov, D., Ma, X., Brot, N., Elkon, K.B., 2002. I-PLA(2) activation during apoptosis promotes the exposure of membrane lysophosphatidylcholine leading to binding by natural immunoglobulin M antibodies and complement activation. J. Exp. Med. 196, 655–665.

Kinjyo, I., Qin, J., Tan, S.Y., Wellard, C.J., Mrass, P., Ritchie, W., Doi, A., Cavanagh, L.L., Tomura, M., Sakaue-Sawano, A., Kanagawa, O., Miyawaki, A., Hodgkin, P.D., Weninger, W., 2015. Real-time tracking of cell cycle progression during CD8+ effector and memory T-cell differentiation. Nat. Commun. 6, 6301.

Lajoie, P., Nabi, I.R., 2010. Lipid rafts, caveolae, and their endocytosis. International Review of Cell and Molecular Biology 282, 135–163.

Liao, Y., Smyth, G.K., Shi, W., 2013. featureCounts: an efficient general purpose program for assigning sequence reads to genomic features. Bioinformatics 30, 923–930.

Lobb, C.J., Olson, M.O., Clem, L.W., 1984. Immunoglobulin light chain classes in a teleost fish. J. Immunol. 132, 1917–1923.

Love, M.I., Huber, W., Anders, S., 2014. Moderated estimation of fold change and dispersion for RNA-seq data with DESeq2. Genome Biol. 15, 550.

Manganelli, V., Capozzi, A., Recalchi, S., Signore, M., Mattei, V., Garofalo, T., Misasi, R., Degli Esposti, M., Sorice, M., 2015. Altered traffic of cardiolipin during apoptosis: exposure on the cell surface as a trigger for "antiphospholipid antibodies. Journal of Immunology Research, 847985.

Miller, N.W., Bly, J.E., van Ginkel, F., Ellsaesser, C.F., Clem, L.W., 1987. Phylogeny of lymphocyte heterogeneity: identification and separation of functionally distinct subpopulations of channel catfish lymphocytes with monoclonal antibodies. Dev. Comp. Immunol. 11, 739–747.

Miller, N.W., Chinchar, V.G., Clem, L.W., 1994a. Development of leukocyte cell lines from the channel catfish (Ictalurus punctatus). J. Tissue Cult. Methods 16, 117–123.

Miller, N.W., Rycyzyn, M.A., Wilson, M.R., Warr, G.W., Naftel, J.P., Clem, L.W., 1994b. Development and characterization of channel catfish long term B cell lines. J. Immunol. 152, 2180–2189.

Patil, V.S., Madrigal, A., Schmiedel, B.J., Clarke, J., O'Rourke, P., de Silva, A.D., Harris, E., Peters, B., Seumois, G., Weiskopf, D., Sette, A., Vijayanand, P., 2018. Precursors of human CD4(+) cytotoxic T lymphocytes identified by single-cell transcriptome analysis. Science Immunology 3.

Pereiro, P., Romero, A., Díaz-Rosales, P., Estepa, A., Figueras, A., Novoa, B., 2017. Nucleated teleost erythrocytes play an nk-lysin- and autophagy-dependent role in antiviral immunity. Front. Immunol. 8, 1458.

Segawa, K., Nagata, S., 2015. An apoptotic 'eat me' signal: phosphatidylserine exposure. Trends Cell Biol. 25, 639–650.

Shen, L., Stuge, T.B., Evenhuis, J.P., Bengtén, E., Wilson, M., Chinchar, V.G., Clem, L.W., Miller, N.W., 2003. Channel catfish NK-like cells are armed with IgM via a putative FcμR. Dev. Comp. Immunol. 27, 699–714.

Sorice, M., Circella, A., Misasi, R., Pittoni, V., Garofalo, T., Cirelli, A., Pavan, A., Pontieri, G.M., Valesini, G., 2000. Cardiolipin on the surface of apoptotic cells as a possible

trigger for antiphospholipids antibodies. Clin. Exp. Immunol. 122, 277–284.
Spencer, D., 2018. Supplemental videos: time-lapse visualization of IgM + and IgM-TS32.15 in the presence of target cells. Mendeley Data v1. https://doi.org/10.17632/btww5mxjxg.1.
Stuge, T.B., Wilson, M.R., Zhou, H., Barker, K.S., Bengtén, E., Chinchar, G., Miller, N.W., Clem, L.W., 2000. Development and analysis of various clonal alloantigen-dependent cytotoxic cell lines from channel catfish. J. Immunol. 164, 2971–2977.
Taylor, E.B., Moulana, M., Stuge, T.B., Quiniou, S.M.A., Bengten, E., Wilson, M., 2016. A leukocyte immune-type receptor subset is a marker of antiviral cytotoxic cells in channel catfish, Ictalurus punctatus. J. Immunol. 196, 2677–2689.
Taylor, E.B., Nayak, D.K., Quiniou, S.M.A., Bengten, E., Wilson, M., 2015. Identification of SHIP-1 and SHIP-2 homologs in channel catfish, Ictalurus punctatus. Dev. Comp. Immunol. 51, 79–87.
Toda, S., Nishi, C., Yanagihashi, Y., Segawa, K., Nagata, S., 2015. Clearance of apoptotic cells and pyrenocytes. Curr. Top. Dev. Biol. 267–295.
Vallejo, A.N., Ellsaesser, C.F., Miller, N.W., Clem, L.W., 1991. Spontaneous development of functionally active long-term monocytelike cell lines from channel catfish. In vitro cellular & developmental biology. Journal of the Tissue Culture Association 27A, 279–286.
van Ginkel, F.W., Miller, N.W., Lobb, C.J., Clem, L.W., 1992. Characterization of anti-hapten antibodies generated in vitro by channel catfish peripheral blood lymphocytes. Dev. Comp. Immunol. 16, 139–151.
Vasconcelos, Z., Muller, S., Guipouy, D., Yu, W., Christophe, C., Gadat, S., Valitutti, S., Dupre, L., 2015. Individual human cytotoxic T lymphocytes exhibit intraclonal heterogeneity during sustained killing. Cell Rep. 11, 1474–1485.
Wang, H., Coligan, J.E., Morse 3rd, H.C., 2016. Emerging functions of natural IgM and its Fc receptor FCMR in immune homeostasis. Front. Immunol. 7, 99.
Wilson, M., Bengten, E., Miller, N.W., Clem, L.W., Du Pasquier, L., Warr, G.W., 1997. A novel chimeric Ig heavy chain from a teleost fish shares similarities to IgD. Proc. Natl. Acad. Sci. U. S. A. 94, 4593–4597.
Wilson, M.R., Zhou, H., Bengtén, E., Clem, L.W., Stuge, T.B., Warr, G.W., Miller, N.W., 1998a. T-cell receptors in channel catfish: structure and expression of TCR alpha and beta genes. Mol. Immunol. 35, 545–557.
Wilson, M.R., Zhou, H., Bengtén, E., Clem, L.W., Stuge, T.B., Warr, G.W., Miller, N.W., 1998b. T-cell receptors in channel catfish: structure and expression of TCR α and β genes. Mol. Immunol. 35, 545–557.
Xiang, J., Wan, C., Guo, R., Guo, D., 2016. Is hydrogen peroxide a suitable Apoptosis inducer for all cell types? BioMed Res. Int. 2016, 1–6.
Yoshida, S.H., Stuge, T.B., Miller, N.W., Clem, L.W., 1995. Phylogeny of lymphocyte heterogeneity: cytotoxic activity of channel catfish peripheral blood leukocytes directed against allogeneic targets. Dev. Comp. Immunol. 19, 71–77.
Zhou, H., Stuge, T.B., Miller, N.W., Bengten, E., Naftel, J.P., Bernanke, J.M., Chinchar, V.G., Clem, L.W., Wilson, M., 2001. Heterogeneity of channel catfish CTL with respect to target recognition and cytotoxic mechanisms employed. J. Immunol. 167, 1325–1332.